



## Original Article

# Gene Expression Analysis Reveals Clinically Significant Genes Associated with Familial Hypercholesterolemia and Atherosclerosis



Kumaran Kasianthan<sup>1</sup>, Janardanan Subramonia Kumar<sup>2</sup> and Kandasamy Nagarajan ArulJothi<sup>1\*</sup> 

<sup>1</sup>Department of Genetic Engineering, College of Engineering and Technology, SRM Institute of Science and Technology, Kattankulathur, Chengalpattu, Tamil Nadu, India; <sup>2</sup>Department of General Medicine, SRM Medical College Hospital and Research Centre, SRM Nagar, Potheri, Chengalpattu, Tamil Nadu, India

Received: November 28, 2023 | Revised: December 28, 2023 | Accepted: February 28, 2024 | Published online: May 15, 2024

### Abstract

**Background and objectives:** Familial hypercholesterolemia (FH) is characterized by an elevated level (>155 mg/dL) of LDL (low-density lipoprotein)-Cholesterol in the blood circulation and is one of the major causes of premature atherosclerotic cardiovascular diseases. The significant genes responsible for this lipid deposition are LDL-Receptor (*LDLR*), Apolipoprotein B-100 (*APOB*), and proprotein convertase subtilisin/kexin type 9 genes (*PCSK9*). Other than these 3 genes, 64 gene loci have been identified as polygenic causes. The aim of the study is to analyze the other genes involved in this condition. This can be obtained using differential expression analysis of the already existing FH mRNA expression dataset.

**Methods:** In this study, three datasets representing the markers of monocyte, T lymphocyte, and iPSC in atherosclerosis and FH were selected from the pool of hypercholesterolemia datasets, and differential expression analysis was done using networkanalyst.ca.

**Keywords:** Familial Hypercholesterolemia; Gene expression; DNA microarray; Network Analyst; Limma; LDL-Cholesterol.

**Abbreviations:** ABC, ATP-binding Cassette; ABCG5, ATP-Binding Cassette Subfamily G Member 5; ABCG8, ATP-Binding Cassette Subfamily G Member 8; AKR1C3, Aldo-Keto Reductase Family 1 Member C3; APOB, Apolipoprotein B; APOE, Apolipoprotein E; BPs, Biological Processes; CC, Cellular Components; CELSR2, Cadherin EGF LAG Seven-Pass G-Type Receptor 2; COPS2, COP9 Signalosome Subunit 2; COX7B, Cytochrome C Oxidase Subunit 7B; CVD, cardiovascular disease; DEGs, differentially expressed genes; FH, familial hypercholesterolemia; GEO, Gene Expression Omnibus; GO, gene ontology; GZMA, Granzyme A; HLA, Human Leukocyte Antigen.; HSD17B3, Hydroxysteroid 17-Beta Dehydrogenase 3; KLRF1, Killer Cell Lectin Like Receptor F1; LDL-C, low-density lipoprotein cholesterol; LDLR, Low-Density Lipoprotein Receptor; LDLRAP1, Low-Density Lipoprotein Receptor Adaptor Protein 1; LY96, Lymphocyte Antigen 96; MA plot, M vs A plot; MCODE, Molecular Complex Detection; MFs, Molecular Functions; MYLIP, Myosin Regulatory Light Chain Interacting Protein; MYO18B, Myosin XVIIIIB; NCOR2, Nuclear Receptor Corepressor 2; NDUFA4, NADH: Ubiquinone Oxidoreductase Subunit A4; NLR, NOD-like receptor; NMD3, Ribosome Exporting Factor; OSM, Oncostatin M; PCSK9, Proprotein Convertase Subtilisin/Kexin Type 9; PEX6, Peroxisomal Biogenesis Factor 6; PL9, Phospholamban (PLN); POLR2A, RNA Polymerase II Subunit A; RPL34, Ribosomal Protein L34; RPL9, Ribosomal Protein L9; RPS9, Ribosomal Protein S9; RSL24D1, Ribosomal L24 Domain Containing 1; TCN1, Transcobalamin 1; TLR4, Toll-like receptor 4; XK, X-Linked Kx Blood Group; YOD1, Deubiquitinase OTU1; ZNHIT3, Zinc Finger HIT-Type Containing 3.

\***Correspondence to:** Kandasamy Nagarajan ArulJothi, Department of Genetic Engineering, College of Engineering and Technology, SRM Institute of Science and Technology, Kattankulathur, Chengalpattu, Tamil Nadu 603203, India. ORCID: <https://orcid.org/0000-0002-1514-9911>. Tel: +91-7854206014, E-mail: [aruljotn@srmist.edu.in](mailto:aruljotn@srmist.edu.in) or [aruljothi@biotech@gmail.com](mailto:aruljothi@biotech@gmail.com)

**How to cite this article:** Kasianthan K, Kumar JS, ArulJothi KN. Gene Expression Analysis Reveals Clinically Significant Genes Associated with Familial Hypercholesterolemia and Atherosclerosis. *Gene Expr* 2024;000(000):000–000. doi: 10.14218/GE.2023.00184.

**Results:** The monocyte and t-lymphocytes datasets each had 743 differentially expressed genes (DEGs), while the iPSCs dataset contained 691 DEGs. *RPS7*, *AKRIC3*, *PL9*, and *OSM* are among the genes that are expressed in the majority of Gene ontology annotations.

**Conclusions:** According to the findings, genes with varied levels of expression are associated with a variety of functions, including membrane transport, ubiquitin-protein ligase activity, the *COP9* signalosome complex, the mitochondrial respiratory chain, and copper metabolism. Analyzing these critical genes lays the groundwork for investigating potential therapeutic targets that could alleviate the impact of cardiovascular disease in individuals diagnosed with FH.

### Introduction

Familial hypercholesterolemia (FH) is a genetic disorder characterized by elevated levels of low-density lipoprotein cholesterol (LDL-C) in the bloodstream. This condition is inherited in an autosomal co-dominant pattern. The observed phenomenon can be attributed to a genetic mutation in the lipid metabolizing genes, which are LDL receptor (*LDLR*), apolipoprotein B (*APOB*), and

proprotein convertase subtilisin/kexin type 9 (*PCSK9*). A total of 64 additional gene loci have been implicated in polygenic etiology.<sup>1</sup> According to the findings of epidemiological research, the heterozygous variant of FH, known as HeFH, demonstrates a prevalence of approximately 1 in every 300 individuals.<sup>2,3</sup>

Conversely, the homozygous form of FH, known as HoFH, demonstrates a prevalence of approximately 1 in every 500 individuals. In instances of homozygous familial FH, individuals have symptoms characterized by plasma LDL levels that are twice as detrimental compared to heterozygote patients. The disorder arises from genetic anomalies that affect the gene responsible for regulating the cellular receptor for LDL. As a result, there is an interruption in the process of attaching or absorbing this lipoprotein. Individuals diagnosed with HoFH frequently demonstrate a restricted reaction to existing treatments, owing to decreased functionality of the LDL receptor.<sup>4,5</sup> Generally, LDL readings of 150 mg/dL are typically considered normal for adults in good health. Nevertheless, current guidelines recommend that those at high risk of cardiovascular disease (CVD) reduce their LDL levels to 70 mg/dL. It is advisable to strive for a minimum reduction of 30% in LDL-C levels. Individuals at high risk should aim for a decrease of at least 50%.<sup>2,6,7</sup> This vascular intima disease is characterized by the presence of intimal plaques, which have the potential to impact both the aorta and coronary arteries. These plaques form when tiny cholesterol crystals accumulate in the intima and smooth muscle.<sup>8</sup> Compared to those with normal LDL cholesterol levels, individuals with this disorder are three to ten times more likely to develop early asymptomatic atherosclerotic cardiovascular disease.<sup>9,10</sup> If untreated, young adult FH patients (20–40 years old) have a 100-fold increased risk of disease mortality. Commonly, the first-line therapies consist of cholesterol-lowering drugs including statins, ezetimibe, and PCSK9 inhibitors. Nevertheless, their efficacy is constrained by the diminished functionality of LDLR. Despite the recent noteworthy advancements in therapeutic interventions for atherosclerosis, the primary hurdle that persists is identifying and elucidating biomarkers for early detection and the precise molecular mechanisms underlying the disease. When a condition occurs, multiple underlying physiological processes occur throughout the body. Examining the underlying genes responsible prior to treatment is crucial in this instance. This is why many treatments frequently fail, due to insufficient understanding of the genes involved. Within the current medical context, it is evident that a standardized approach to patient treatment is no longer adequate. Hence, it is imperative to provide customized treatment for each individual, also known as individualized treatment, personalized. The investigation of multi-dimensional data necessitates the application of unconventional methodologies and technologies. Various biomarker approaches are currently being investigated as potential diagnostic tests for atherosclerosis and related disorders. Recently, data from gene expression microarrays in atherosclerosis have been employed to identify biomarkers, repurpose drugs already in use, and uncover new therapeutic targets.<sup>11,12</sup> A comparative analysis of the changes in gene expression observed in individuals diagnosed with atherosclerosis in contrast to those observed in individuals without the disease shows promise in elucidating the underlying pathophysiological mechanisms that contribute to dysfunction and identifying a distinct gene expression pattern associated with the disease. Pathway enrichment analysis is a potent method for data analysis in genomics, primarily gene expression research. The software analyzes a wide range of omics data types, including protein-protein interactions and genomics,

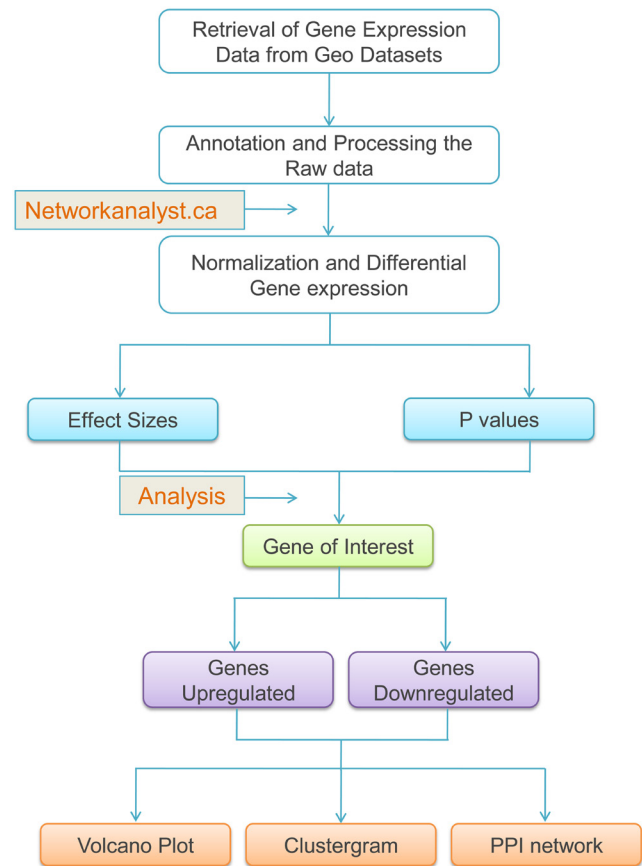


**Fig. 1. Graphical representation of differential gene expression analysis of familial hypercholesterolemia (FH) and atherosclerosis datasets.** GEO, Gene Expression Omnibus; PPI, Protein-Protein Interaction.

proteomics, and metabolomics. This primarily entails analyzing biological aspects that are similar to the collection of features that the researcher thought was important, which are typically features with significant expression changes or differentially expressed genes (DEGs).<sup>13</sup>

Gene set enrichment analysis is a widely used method for interpreting the findings of gene expression research. This method is predicated on the functional annotation of genes expressed at different levels. This strategy's applicability lies in determining whether the differentially expressed genes are associated with a specific biological activity or molecular function. Almost all transcriptome analyzes include enrichment analysis, which provides a valuable overview of the processes or functions connected to the genes of interest.<sup>14</sup> With a user-friendly online interface, bench researchers can use networkanalyst.ca, a full-featured web-based application, to perform a variety of simple and complex meta-analyses of gene expression data. In order to enhance our comprehension of fundamental biological mechanisms, we conducted comprehensive research investigations as mentioned in Fig. 1, that yielded substantial datasets of genes. The genes, which exhibit varying degrees of activity under different circumstances, are examined to derive a functional profile of the group of genes.<sup>15,16</sup> In this study, we utilized networkanalyst.ca, a platform that employs limma to analyze the differential expression of genes in individuals with FH and atherosclerosis. Through analysis, we can identify the

genes that have a key role in our specific ailment, offering a fresh perspective for diagnosis and study.

## Methods

### Data retrieval

The GEO (Gene Expression Omnibus) database provides web-based technical assistance for retrieving, identifying, and analyzing gene expression patterns submitted to the database. Three atherosclerosis and FH datasets were chosen from the pool of hypercholesterolemia datasets examined within the GEO collection. The datasets that have been obtained for analysis include GSE6054 (Monocytes of patients with FH show alterations in cholesterol metabolism), GSE6088 (Imprints of atherosclerosis are present in circulating T cells of patients with FH), and GSE75545 (Urine-sample-derived human induced pluripotent stem cells as a model to study PCSK9-mediated autosomal dominant hypercholesterolemia)

To analyze the data in networkanalyst.ca, a dataset must include a gene name file containing the matching analysis code and gene code for each gene. The gene code should include the official gene symbol, Ensemble gene ID, GenBank ID, Ref Seq ID, Entrez ID, Ensemble ID, and UniProt Accession ID. There are downloadable files with Affymetrix human genome and Agilent Human 18 cDNA microarray data. Additionally, there is another file that includes the aforementioned code and the accompanying empirical data for the research investigation. When selecting datasets, it is crucial to verify that they include the required data and genetic code. Alternatively, the software will reject them. Furthermore, the dataset must include information regarding the sample type, specifically differentiating between patient samples and control samples. Upon thorough examination, we have determined that there are only three datasets that satisfy the criteria for investigating FH.

### Data processing

All of the retrieved raw data were converted to an Excel file, and the entries in the Excel file were inspected for unnecessary information in the series matrix file, such as RefSeq, control type, UniGene ID, ensemble ID, accession string, chromosome number, gene ontology (GO) ID, and sequence data, and eliminated. Only the ID and Gene symbol are necessary. These unnecessary additions render the final document incomprehensible. The platform files containing the gene expression datasets were also examined for undesired elements and deleted; the two files were then integrated and processed jointly using the ID data.

### Normalization and differential expression

Using Network analysis, we may rapidly and easily browse sizable complex gene expression data sets to identify essential characteristics, patterns, functions, and relationships that inspire the development of novel biological ideas.<sup>17</sup> The purpose is to standardize the data by eliminating duplicate data, as the same information will be recorded in multiple databases. The main objective of the normalization is to get the database organized. The first step is to eliminate any duplicate data from the data set. This modifies the database to eliminate duplicated entries, missing data, and errored information. It is easier to evaluate and clean up the data if we try to eliminate them from the database. This will occur in a database through the log<sub>2</sub> normalization procedure. Based on the well-established linear model such as limma, Network-Analyst

can conduct extremely complicated Differential expressions for the entered microarray datasets.<sup>18</sup>

### Interpretation of DEGs

The findings of gene expression analysis revealed information concerning the genes as well as the expression levels of each gene in question. These data were manually input into an Excel spreadsheet, which was then used to categorize the data based on whether regulation increased or decreased. The relative depiction of mean expression levels, log fold changes, and corrected *p*-values can benefit from the use of both MA plots and volcano plots. Both plots can be helpful. To further comprehend the findings, we utilized the Volcano Plot in conjunction with the MA plot. The MA plot and the volcano were both created using the ORIGIN software with DEG data. The x-axis of the volcano plot represented the log<sub>2</sub> fold change, while the y-axis represented the log<sub>2</sub> of the *p*-value. The log<sub>2</sub> fold change was plotted along the y-axis in the MA plot, while the log<sub>2</sub>Exp was plotted along the x-axis. Both of these measurements are expressed as percentages.<sup>19</sup>

### Network construction

The three major processes of network analysis include data processing to identify significant genes, network construction to map, create, and improve networks, and network analysis and visualization. The direct or indirect links between expressed proteins can be researched more effectively with the assistance of the STRING website.<sup>20,21</sup> The DEGs that resulted from the events that were described. The PPI networks exhibited a maximum enrichment *p*-value at  $1.0 \times 10^{-16}$  and a minimal average local clustering coefficient value of higher than 0.4. The network was constructed using nodes with a confidence score higher than 0.4 and a maximum number of extra interactions of 10.

The Molecular Complex Detection (MCODE) Cytoscape plugin was utilized to find clusters inside the PPI networks.<sup>22</sup> The parameters for these calculations were as follows: a k-core value of 2, a node score of 0.2, a degree cutoff of 2, and a network depth of 100. The data collected for this study was presented using an illustration of a network structure. We then utilized the Cytoscape plugin to focus our search for hub genes on those with high MCODE scores (more than 5). In addition, well-established FH candidate genes (*LDLR*, *LDLRAP1*, *PCSK9*, *APOB*, *ABCG5*, *APOA1*, and *ABCG8*) were utilized to construct subnetworks with the primary genes.<sup>23</sup>

### GO annotation

The Enrichr web server, located at <https://maayanlab.cloud/Enrichr>, was provided with the overexpressed protein set.<sup>24,25</sup> The Enrichr program offers a GO analysis feature that allows for the examination of the biological implications of protein-protein interaction across multiple dimensions, including Biological Processes (BPs), Cellular Components (CC), Molecular Functions (MFs), and Reactome. This analysis focuses on subnetworks with a *p*-value below 0.05, which yield valuable scientific insights. A thorough examination of the GO annotation was performed employing the Enrichment Analysis Visualization Appyter to determine the comparative importance of discrete terms. The Appyter is a tool that expedites the generation of scatterplots, bar charts, hexagonal canvases, Manhattan plots, and volcano plots, thereby facilitating their construction. Following that, the results will be examined at how each gene set is expressed in different disease-related biological pathways, the pathway's activity score will be estimated using samples, and the critical pathways will be found in

a pathway network. The biological pathway serves as the foundation for explaining human activity and provides information on the pathway's gene similarity (Fig. 1).

## Results

### Interpretation of DEGs

The obtained datasets GSE6054 (Monocytes of patients with FH show alterations in cholesterol metabolism), GSE6088 (Imprints of atherosclerosis are present in circulating T cells of patients with FH and GSE75545 (Urine-sample-derived human induced pluripotent stem cells as a model to study PCSK9-mediated autosomal dominant hypercholesterolemia) were analyzed using network-analyst.ca.<sup>26</sup> The differentially expressed genes are *HLA-DRB5*, *WARS2*, *NLRP2*, *HERC2P7*, *PEX6*, *OSM*, *HSD17B3*, *MYO18B*, *RGPD4-AS1*, *CYS1*, *FAM184B*, *MYOM2*, *LINC00958*, *CLDN8*, *LINC00644*, *ZNHIT3*, *LY96*, *CD52*, *CLIC3*, *NDUFA4*, *LAIR2*, *EVI2A*, *RSL24D1*, *RPL34*, *KLRF1*, *GZMA*, *AKR1C3*, *COMMD6*, *COPS2*, *COX7B*, *TCN1*, *RPS7*, *RPL9*, *YOD1*, *RNF182*, and *XK* and they play vital roles in various cellular functions (Table 1). *HLA-DRB5* is an Human Leukocyte Antigen (HLA) system component that regulates the immunological response. *HLA* genes produce proteins that aid the immune system in differentiating between the body's proteins and those produced by external invaders such as viruses and bacteria. *WARS2* is a gene that encodes tryptophanyl-tRNA synthetase, a component of mitochondrial protein synthesis. *NLRP2* is a member of the NLR family that regulates inflammation and immunological reactions. It is understood to play a role in the synthesis of inflammasomes. Participates in peroxisome biogenesis (*PEX6*), and the rare congenital condition Zellweger syndrome is linked to mutations in this gene. The gene *OSM* encodes the oncostatin M, a protein involved in a variety of biological processes such as liver regeneration, inflammation, and tumor cell growth suppression. *HSD17B3* encodes an enzyme required for producing androgens, the male sex hormones. Myosin, a protein usually involved in several cellular functions, including motility, polarity, and division, is encoded by the gene *MYO18B*. Associated with cystinuria, a condition in which specific amino acids, especially cystine, move abnormally in the kidneys. *CLDN8* is a member of the claudin family and contributes to the cells. *ZNHIT3* is a member of the HIT zinc finger protein family; although its precise function is still unknown, HIT proteins are typically implicated in nucleic acid binding. *LY96* generates a protein that aids in the immune system's identification of bacterial compounds, triggering an inflammatory reaction. *CD52* codes for a protein targeted for various leukemia and multiple sclerosis therapies. *CLIC3* is a member of the family of chloride intracellular channels, which is involved in the transport of chloride ions into cells. *NDUFA4* encodes a Complex I subunit, which is part of the mitochondrial respiratory chain. *LAIR2* is an immune cell receptor that aids in controlling immunological reactions. *EVI2A* may have a role in immune cell development, while its exact function is uncertain. The ribosomal proteins, known as *RSL24D1*, *RPL34*, *RPS7*, and *RPL9*, are essential parts of ribosomes, the organelles responsible for protein synthesis in cells. *KLRF1* is an immune system protein identified in natural killer cells. Granzyme A, an enzyme secreted by cytotoxic T cells and natural killer cells to target and eliminate infected or damaged cells, is encoded by the gene *GZMA*. *AKR1C3* mediates prostaglandin and steroid metabolism. The genes *COMMD6*, *COPS2*, *COX7B*, *YOD1*, *RNF182*, and *XK* participate in a variety of processes, including membrane transport, ubiquitin-

protein ligase activity, COP9 signalosome complex, mitochondrial respiratory chain, and copper metabolism.

Another commonly used method for comparing the two treatment conditions is the evaluation of the adjusted *p*-value to the logarithm of the fold change. The depicted diagram is commonly referred to as a volcano plot, owing to its resemblance to an erupting volcano, wherein clusters of data points are observed near the origin while exhibiting a dispersing pattern as they move away from this central position. Volcano plots are graphical representations that exhibit the statistical significance of the disparity to the extent of difference for each gene in the comparison. Typically, this is accomplished by employing the negative logarithm to base 10 for statistical significance and the logarithm to base 2 for fold change (Fig. 2). A broader distribution indicates a greater degree of disparity in gene expression between the two treatment groups. The occurrence of a volcano plot exhibiting a majority, or the entirety, of data points being densely clustered in proximity to the origin is a relatively infrequent phenomenon. MA plots exhibit the capacity to solely compare two distinct treatment conditions simultaneously.

Nevertheless, it is feasible to consolidate all pairwise comparisons about this specific illustration into a matrix configuration, allowing for the simultaneous representation of all conceivable combinations. This visualization facilitates the simultaneous monitoring of all pairwise comparisons between fold change and mean expression. Presents a methodology to ascertain the relative similarities or dissimilarities between treatment comparisons based on log-fold change and mean expression level. This approach, akin to the other matrix alternatives, allows users to visually depict their treatment-based comparisons. Genes exhibiting a log<sub>2</sub>(Fold Change) value exceeding zero can be classified as upregulated genes, while genes with a log<sub>2</sub>(Fold Change) value below zero can be categorized as downregulated. The nodes exhibiting a red coloration demonstrate a significant upregulation, whereas the nodes in yellow indicate a significant downregulation.

### Network construction

The findings of the pathway enrichment analysis revealed that the Module has 32 nodes and 68 edges. These nodes and edges are largely concerned with the control of differentially expressed genes implicated in the development of atherosclerosis. Within the realm of protein networks, it is observed that protein partners within a cluster exhibit comparable functional attributes. Furthermore, these clusters rely heavily on hub genes, which are biologically interconnected nodes. The MCODE plugin, which is integrated into the Cytoscape software, detects and delineates clusters within a protein network. The MCODE cluster was subsequently augmented with eight prominent genes involved in lipid metabolism, namely *APOB*, *LDLR*, *LDLRAP1*, *ABCA1*, *PCSK9*, *ABCG8*, *APOA1*, *APOC3*, and *ABCG5*, in order to expand the protein-protein interaction network for further analysis. The FH nodes interacting with DEG edges possess an average STRINGDB interaction. The *APOB* binds to *XK* and *LY96*, *APOA1* binds to *LY96*, and the *PCSK9* binds to the *OSM* gene. GO annotations contain biological information about genes and the proteins they produce (Figs. 3 and 4).

### GO and the annotation

The enricher demonstrates that the enrichment terms for the biological process are sterol transport (GO: 0015918), cholesterol homeostasis (GO: 0042632), and sterol homeostasis (GO: 0035092). Cholesterol Transfer Activity (GO: 0120020), Sterol Transfer

**Table 1. Interpretation of differentially expressed genes obtained from datasets GSE6054 (Monocytes of patients with familial hypercholesterolemia show alterations in cholesterol metabolism), GSE6088 (Imprints of atherosclerosis are present in circulating T cells of patients with familial hypercholesterolemia) and GSE75545 (Urine-sample-derived human induced pluripotent stem cells as a model to study PCSK9-mediated autosomal dominant hypercholesterolemia) analyzed using networkanlayst.ca**

EntrezID	adj.P.Val	p-Value	t	B	logFC	Symbols	Name
Monocyte (GSE6054)							
84700	0.013008	0.000905	4.7528	1.5037	2.4492	<i>MYO18B</i>	Myosin XVIIIIB
1.02 × 10 <sup>8</sup>	0.046545	0.001005	3.7765	-0.72929	2.1865	<i>LINC00644</i>	Long intergenic non-protein coding RNA 644
192668	0.025636	0.000317	4.2456	0.34062	2.0798	<i>CYS1</i>	Cystin 1
9073	0.036811	0.000647	3.9562	-0.32126	2.0366	<i>CLDN8</i>	Claudin 8
729121	0.022197	0.000254	4.3352	0.54608	1.7591	<i>RGPD4-AS1</i>	RGPD4 antisense RNA 1 (head-to-head)
1.01E+08	0.030334	0.000453	4.1003	0.007688	1.515	<i>LINC00958</i>	Long intergenic non-protein coding RNA 958
27146	0.026046	0.000327	-4.2326	0.31073	-1.7116	<i>FAM184B</i>	Family with sequence similarity 184 member B
3293	0.009849	0.000519	-4.9792	2.0207	-1.9794	<i>HSD17B3</i>	Hydroxysteroid 17-beta dehydrogenase 3
9172	0.03027	0.000447	-4.1062	0.021258	-2.0318	<i>MYOM2</i>	Myomesin 2
T lymphocyte (GSE6088)							
6947	0.3014	0.014387	-2.8309	-2.8318	-1.0073	<i>TCN1</i>	Transcobalamin 1
9022	0.20729	0.001842	-3.9135	-1.0713	-1.0099	<i>CLIC3</i>	Chloride intracellular channel 3
9318	0.2472	0.007666	-3.1611	-2.2919	-1.015	<i>COPS2</i>	COP9 signalosome subunit 2
3001	0.24454	0.006849	-3.2201	-2.1951	-1.0251	<i>GZMA</i>	Granzyme A
6133	0.3272	0.020406	-2.6466	-3.1303	-1.0317	<i>RPL9</i>	Ribosomal protein L9
1043	0.20262	0.001707	-3.9542	-1.0067	-1.0424	<i>CD52</i>	CD52 molecule
170622	0.24454	0.007035	-3.2061	-2.2181	-1.0622	<i>COMMMD6</i>	COMM domain containing 6
3904	0.23062	0.004078	-3.4922	-1.7503	-1.0823	<i>LAIR2</i>	Leukocyte-associated immunoglobulin-like receptor 2
6201	0.32452	0.019401	-2.6733	-3.0872	-1.0851	<i>RPS7</i>	Ribosomal protein S7
221687	0.47346	0.063946	-2.0282	-4.09	-1.0976	<i>RNF182</i>	Ring finger protein 182
9326	0.20034	0.000504	-4.6202	0.020066	-1.1045	<i>ZNHIT3</i>	Zinc finger HIT-type containing 3
2123	0.23062	0.00412	-3.4868	-1.7591	-1.1093	<i>EVI2A</i>	Ecotropic viral integration site 2A
55432	0.43923	0.051957	-2.1434	-3.9183	-1.1175	<i>YOD1</i>	YOD1 deubiquitinase
6164	0.23746	0.005617	-3.324	-2.025	-1.1277	<i>RPL34</i>	Ribosomal protein L34
51187	0.23062	0.004557	-3.4338	-1.8455	-1.1559	<i>RSL24D1</i>	Ribosomal L24 domain containing 1
23643	0.20034	0.000721	-4.4216	-0.27935	-1.1582	<i>LY96</i>	Lymphocyte antigen 96
51348	0.24403	0.006614	-3.2384	-2.1651	-1.2234	<i>KLRF1</i>	Killer cell lectin-like receptor F1
4697	0.22389	0.003022	-3.6503	-1.4938	-1.2324	<i>NDUFA4</i>	NDUFA4 mitochondrial complex associated
1349	0.27484	0.010668	-2.9879	-2.5755	-1.2459	<i>COX7B</i>	Cytochrome c oxidase subunit 7B
8644	0.24454	0.006927	-3.2142	-2.2048	-1.3589	<i>AKR1C3</i>	Aldo-keto reductase family 1 member C3
7504	0.48675	0.06987	-1.9786	-4.1627	-1.3766	<i>XK</i>	X-linked Kx blood group
iPSC (GSE75545)							
3127	0.055267	3.92E-06	8.9974	-1.6805	1.2	<i>HLA-DRB5</i>	Major histocompatibility complex, class II, DR beta 5
55655	0.33643	4.78E-05	-6.7624	-2.019	-2.5227	<i>NLRP2</i>	NLR family pyrin domain containing 2

iPSC, induced pluripotent stem cells.

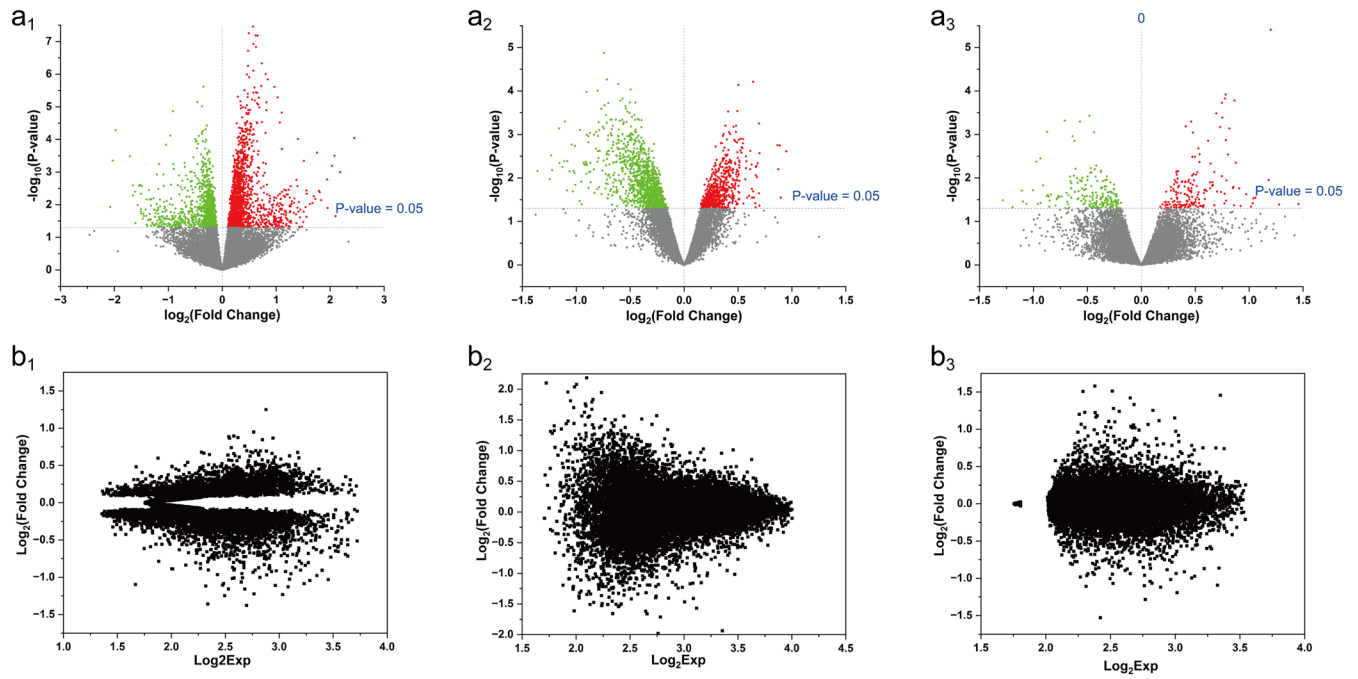


**Fig. 2. The interpretations of Differential expression results retrieved from network analyst tool.** (a) The volcano plot of monocyte—GSE6054 (Monocytes of patients with familial hypercholesterolemia show alterations in cholesterol metabolism), T-lymphocyte - GSE6088 (Imprints of atherosclerosis are present in circulating T cells of patients with Familial Hypercholesterolemia) and hematopoietic cells—GSE75545 (Urine-sample-derived human induced pluripotent stem cells as a model to study PCSK9-mediated autosomal dominant hypercholesterolemia) in FH, Atherosclerosis, and (b) The MA plot of monocyte, T-lymphocyte and hematopoietic cells in FH and Atherosclerosis. FH, familial hypercholesterolemia; MA plot, M vs A plot.

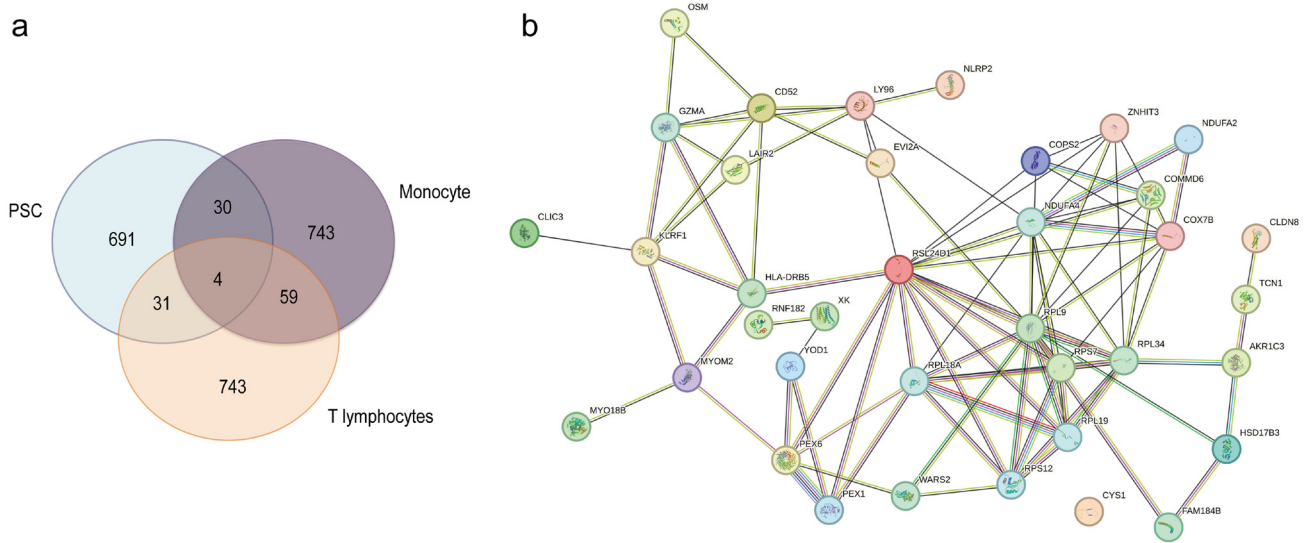


**Fig. 3. Interpretation of commonly expressed genes from all datasets.** (a) The Venn diagram involves the DEGs in monocyte, T-lymphocyte and hematopoietic cells in FH, Atherosclerosis, and (b) The PPI network analysis of the obtained overexpressed genes from the 3 datasets. AKR1C3, Aldo-Keto Reductase Family 1 Member C3; CD52, CD52 Molecule; CLDN8, Claudin 8; CLIC3, Chloride Intracellular Channel 3; COMM6, COMM Domain Containing 6; COPS2, COP9 Signalosome Subunit 2; COX7B, Cytochrome C Oxidase Subunit 7B; CYS1, Cystin 1; DEGs, differentially expressed genes; EVI2A, Ecotropic Viral Integration Site 2A; FAM184B, Family with Sequence Similarity 184 Member B; GZMA, Granzyme A; RPL9, Ribosomal Protein L9; HLA-DRB5, Major Histocompatibility Complex, Class II, DR Beta 5; HSD17B3, Hydroxysteroid 17-Beta Dehydrogenase 3; KLRF1, Killer Cell Lectin Like Receptor F1; LAIR2, Leukocyte-Associated Immunoglobulin-Like Receptor 2; LINC00644, Long Intergenic Non-Protein Coding RNA 644; LINC00958, Long Intergenic Non-Protein Coding RNA 958; LY96, Lymphocyte Antigen 96; MYO18B, Myosin XVIIIb; MYO2, Myomesin 2; NDUFA4, NADH:Ubiquinone Oxidoreductase Subunit A4; NLRP2, NLR Family Pyrin Domain Containing 2. FH, familial hypercholesterolemia; PPI, Protein-Protein Interaction.; RGPL4-AS1, RGPL4 Antisense RNA 1; RNF182, Ring Finger Protein 182; RPL34, Ribosomal Protein L34; RPS7, Ribosomal Protein S7; RSL24D1, Ribosomal L24 Domain Containing 1; TCN1, Transcobalamin 1; XK, XK, Kell Blood Group Complex Subunit-Related Family, Member 3; YOD1, Deubiquitinase YOD1; ZNHIT3, Zinc Finger HIT-Type Containing 3.

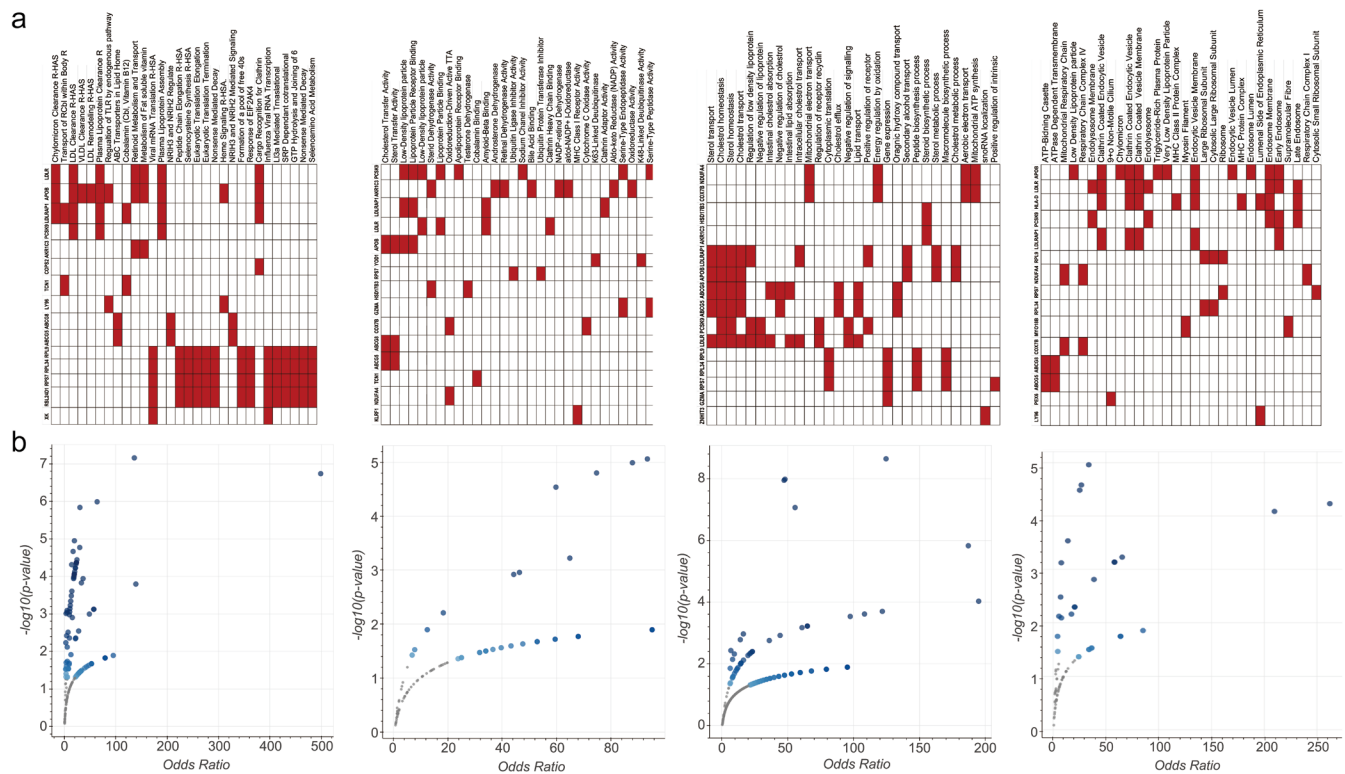


**Fig. 4. Gene Ontology (GO) annotation of the genes.** (a) The Clustergram of Enrich tool provides a graphical representation of the enrichment patterns of FH genes across various GO keywords. These terms include biological processes (BP), molecular function (MF), and cellular components (CC). The genes provided as input are shown in the horizontal columns, and the matrices indicate the enriched phrases connected with that gene and (b) the statistical importance of gene sets is represented by the Bokeh plots that are generated by the Enrich tool. These plots show each data point as a dot that is plotted against the odds ratios. The odds ratios and the negative logarithm of the  $p$ -values are shown along the x-axis, while the  $p$ -values are plotted along the y-axis. ABCG5, ATP-Binding Cassette Subfamily G Member 5; ABCG8, ATP-Binding Cassette Subfamily G Member 8; AKR1C3, Aldo-Keto Reductase Family 1 Member C3; APOB, Apolipoprotein B; COPS2, COP9 Signalosome Subunit 2; COX7B, Cytochrome C Oxidase Subunit 7B; FH, familial hypercholesterolemia.; GZMA, Granzyme A; HLA, Human Leukocyte Antigen; HSD17B3, Hydroxysteroid 17-Beta Dehydrogenase 3; KLRF1, Killer Cell Lectin Like Receptor F1; LDLR, Low-Density Lipoprotein Receptor; LDLRAP1, Low - Density Lipoprotein Receptor Adaptor Protein 1; LY96, Lymphocyte Antigen 96; MYO18B, Myosin XVIIIb; NDUFA4, NADH:Ubiquinone Oxidoreductase Subunit A4; PCSK9, Proprotein Convertase Subtilisin/Kexin Type 9; PEX6, Peroxisomal Biogenesis Factor 6; RPL34, Ribosomal Protein L34; RPL9, Ribosomal Protein L9; RPS9, Ribosomal Protein S9; RSL24D1, Ribosomal L24 Domain Containing 1; TCN1, Transcobalamin 1; XK, X-Linked Kx Blood Group; YOD1, Deubiquitinase OTU1; ZNHIT3, Zinc Finger HIT-Type Containing 3.

Activity (GO:0120015), and Low-Density Lipoprotein Particle Receptor Binding (GO:0050750) are the enrichment terms from Molecular Function. Similar to CC, the enrichment terms are ATP-binding Cassette (ABC) Transporter Complex (GO:0043190), Clathrin-Coated Endocytic Vesicle Membrane (GO:0030669), and Clathrin-Coated Endocytic Vesicle (GO:0045334). The primary enrichment terms in Reactome include Chylomicron Clearance R-HAS ( $p$ -value >0.01, Fig. 5).<sup>27</sup>

**Discussion**

FH is distinguished by an elevated concentration of low-density lipoprotein cholesterol (LDL-C) in the bloodstream, which promotes the advancement of atherosclerosis. Atherosclerosis is widely recognized as a prominent risk factor for the development of coronary artery diseases, heart attacks, and strokes.<sup>28</sup> An excessive amount of LDL particles leads to fibrous plaques to form in the subendothelial region, resulting in a reduction in a reduction in artery diameter. This constriction can ultimately result in heart ischemia and myocardial infarction. The primary genetic factors responsible for FH are the *LDLR*, *APOB*, and *PCSK9* genes. The

presence of a mutation in the *LDLR* gene impairs the interaction between the LDL receptor protein and the ApoB-LDL complex. Similarly, a mutation in the *APOB* gene prevents the ApoB protein from attaching to either LDL-C or the LDL receptor. The *PCSK9* mutation enhances the degradation of LDL receptors. Mutations in these three genes together lead to elevated levels of LDL-C in the bloodstream. Another gene, *APOE*, participates in the lipophilization pathway and contributes to elevated levels of LDL-C in the bloodstream. The CELSR2 protein is implicated in proteolytic glycosylation, which contributes to elevated levels of LDL-C in the bloodstream. The proper establishment of *HFE*, *NYNRIN*, *MYLIP* with FH has not been completed. In this investigation, we employed an integrated bioinformatics methodology. We utilized various tools to ascertain potential pathways and genes that may significantly impact the progression of FH. Using the Limma expression in networkanalyst.ca, we discovered 743 DEGs in the monocyte and t-lymphocytes datasets and 691 DEGs in the iPSCs dataset. Upregulated genes included *MYO18B*, *LINC00644*, *CYS1*, *CLDN8*, *RGPD4-AS1*, *LINC00958*, and *HLA-DRB5*. Downregulated genes included *FAM184B*, *HSD17B3*, *MYOM2*, *TCN1*, *CLIC3*, *COPS2*, *GZMA*, *RPL9*, *CD52*, *COMMD6*, *LAIR2*,

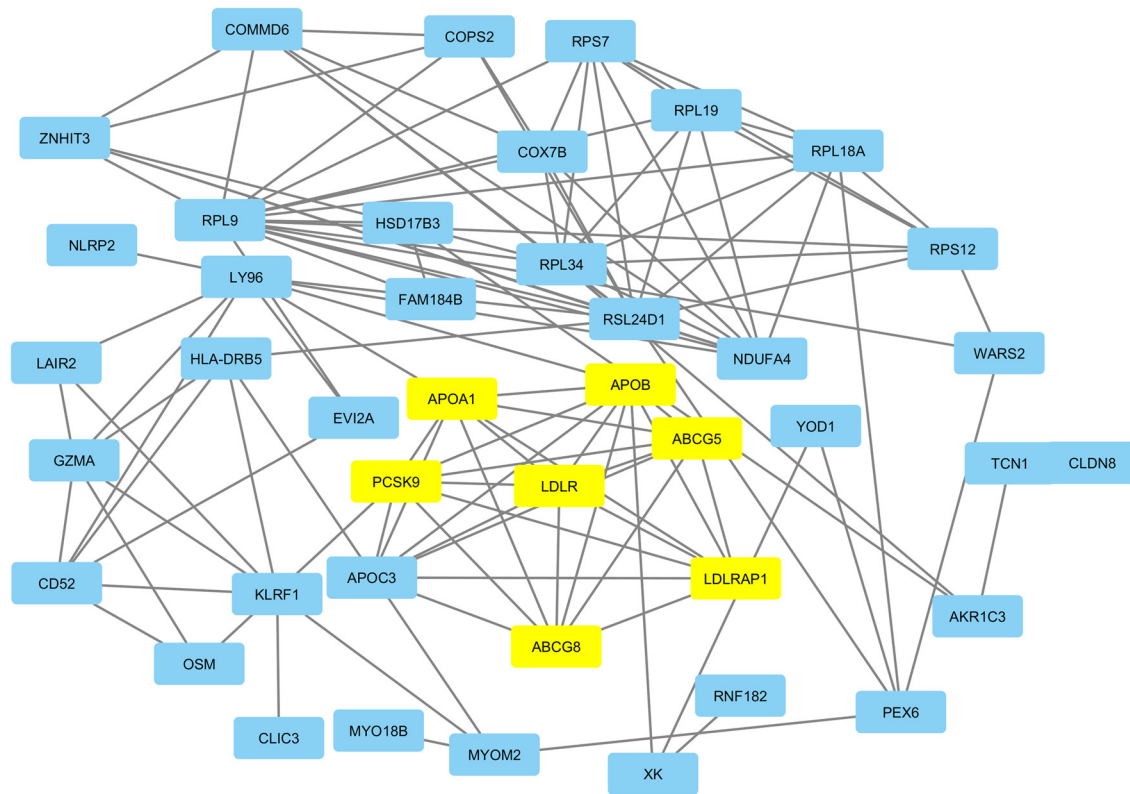


**Fig. 5. PPI network showing interactions between hub genes (Blue) and known FH genes (in yellow) retrieved from Cytoscape.** AKR1C3, Aldo-Keto Reductase Family 1 Member C3; CD52, CD52 Molecule; CLDN8, Claudin 8; CLIC3, Chloride Intracellular Channel 3; COMMD6, COMM Domain Containing 6; COPS2, COP9 Signalosome Subunit 2; COX7B, Cytochrome C Oxidase Subunit 7B; CYS1, Cystin 1; EVI2A, Ecotropic Viral Integration Site 2A; FAM184B, Family with Sequence Similarity 184 Member B; GZMA, Granzyme A RPL9, Ribosomal Protein L9; HLA-DRB5, Major Histocompatibility Complex- Class II- DR Beta 5; HSD17B3, Hydroxysteroid 17-Beta Dehydrogenase 3; KLRF1, Killer Cell Lectin Like Receptor F1; LAIR2, Leukocyte-Associated Immunoglobulin-Like Receptor 2; LINC00644, Long Intergenic Non-Protein Coding RNA 644; LINC00958, Long Intergenic Non-Protein Coding RNA 958; LY96, Lymphocyte Antigen 96; MYO18B, Myosin XVIIIb; MYO2, Myomesin 2; NDUF4A, NADH:Ubiquinone Oxidoreductase Subunit A4; NLRP2, NLR Family Pyrin Domain Containing 2. FH, familial hypercholesterolemia; PPI, Protein-Protein Interaction; RGP4-AS1, RGP4 Antisense RNA 1; RNF182, Ring Finger Protein 182; RPL34, Ribosomal Protein L34; RPS7, Ribosomal Protein S7; RSL24D1, Ribosomal L24 Domain Containing 1; TCN1, Transcobalamin I; XK, Kell Blood Group Complex Subunit-Related Family, Member 3; YOD1, Deubiquitinase YOD1; ZNHIT3, Zinc Finger HIT-Type Containing 3.

*RPS7*, *RNF182*, *ZNHIT3*, *EVI2A*, *YOD1*, *RPL34*, *RSL24D1*, *LY96*, *KLRF1*, *NDUF4A*, *COX7B*, *AKR1C3*, *XK*, and *NLRP2*. The *RSP7* genes were found in all 4 pathways in the ENRICH tool, followed by *AKR1C3*, *PL9* and *OSM* (found in Reactome, BP and CC). Oncostatin M, an IL-6 cytokine, has been demonstrated to potently influence the activation of *LDLR* expression in HepG2 cells through a non-SREBP-mediated route. The transcription factors Egr1 and c/EBP bind to the SIRE region of the promoter, which is located downstream of the SRE-1 region, making it easier to stimulate *LDLR* gene transcription. However, the other 3 genes were not directly involved in the LDL pathway; any connection may be between these three genes and FH, which needs to be focused. According to the Venn diagram, 30 DEGs were common to monocyte and iPSc, 59 DEGs were common in monocyte and t-lymphocyte, and 31 DEGs were common to t-lymphocyte and iPScs. 4 DEGs, *NCOR2*, *NMD3*, *POLR2A* and *RPE*, appeared in all three datasets. The human *NMD3* gene generates proteinaceous nucleolar protein NMD3. It is best recognized for component synthesis and assembly in ribosome biogenesis. *SMRT* (silence mediator for retinoid or thyroid hormone receptors) modulates nuclear receptor-mediated transcriptional activity. Several transcription factors are simultaneously inhibited. *POLR2A* encodes Rpb1, the largest

eukaryotic Pol II component. DNA templates are transcribed into mRNA by RNA polymerase II. The *RPE* gene encodes ribulose-5-phosphate-3-epimerase. In the pentose phosphate pathway, the enzyme produces ribose-5-phosphate, a precursor for nucleotide and nucleic acid biosynthesis. The system creates NADPH, which is required for fatty acid synthesis and reactive oxygen species neutralization.

The PPI network reveals that *PCSK9* interacts with *KLRF1* (a gene that encodes for a receptor that is predominantly expressed on natural killer cells), while *APOB* interacts with Xk and LY96. The *XK* gene encodes the XK protein, a membrane transporter protein predominantly expressed in erythrocytes.<sup>29</sup> The Kell blood group complex encompasses a constituent that is critical in maintaining the integrity and functionality of the erythrocyte membrane. Scientists have recently commenced the analysis of the impact of XK in diverse cardiovascular disorders. For instance, the Toll-like receptor 4 (TLR4) has been associated with lipid metabolism and atherosclerosis, indicating potential implications in the development of CVD.<sup>30</sup> Given the close association between LY96 (MD-2) and TLR4 signaling, it is plausible to hypothesize that it may have an indirect effect on cholesterol metabolism or other related physiological processes.



**Table 2. Functions and location of the identified differentially expressed genes and their role in cardiovascular diseases**

Gene	Function	Location	Relation to cardiovascular disease
<i>KLRF1</i>	Facilitates class 1 MHC receptor activity, carbohydrate binding, transmembrane signaling receptor activity, and plays a role in cell surface receptor signaling pathway	12p13.31	Significant risk factors for cardiovascular disease include the <i>KLRF1</i> gene, which may influence blood pressure and the inflammatory response in the cardiovascular system
<i>Xk</i>	Facilitates protein binding and acts as an adaptor for protein macromolecules. Engaged in the study of AA transport, intracellular calcium and magnesium ion balance, myelination, the regulation of axon diameter and cell size, and muscle fiber development	Xp21.1	The <i>XK</i> gene's involvement in CVD may be connected to its function in preserving the health and functionality of red blood cells. McLeod Syndrome can result from mutations in the <i>XK</i> gene
<i>LY96</i>	Permits the binding of TLR4, coreceptors, LPS, and LPS immune receptors	8q21.11	The <i>LY96</i> gene plays a function in CVD by inducing inflammatory processes that aid in the formation and advancement of atherosclerosis
<i>AKRIC3</i>	It carries out prostaglandin synthase functions	10p15.1	The <i>AKRIC3</i> gene interacts with signaling molecules linked to cardiac hypertrophy, cystic fibrosis, and apoptosis, which may contribute to the onset and progression of CVD
<i>OSM</i>	Controls the function of neurons	22q12.2	<i>OSM</i> may aid in the development of atherosclerotic calcification by promoting osteoblastic differentiation of vascular smooth muscle cells via the JAK3/STAT3 pathway
<i>NCOR2</i>	Control B cell proliferation and preserve genomic integrity	12q24.31	The <i>NCOR2</i> gene plays a role in CVD by controlling lipid metabolism, modifying inflammation, and affecting heart function
<i>NMD3</i>	Serves as an adapter to allow the 60S ribosomal subunit to be exported from the nucleus	3q26.1	<i>NMD3</i> is involved in pathogenesis of cellular tissue in Heart walls
<i>POLR2A</i>	Interacts with <i>CREB1</i> to inhibit osteoclastic bone resorption and prevent osteoporosis	17p13.1	The biggest subunit of RNA polymerase II, <i>POLR2A</i> , is encoded and is involved in the transcription of many different genes. Dysregulation of the <i>POLR2A</i> gene can affect the expression of genes linked to cardiovascular disease and atherosclerosis
<i>RPE</i>	The visual cycle involves the following processes: phagocytosis of shed photoreceptor membranes; re-isomerization of all-trans-retinal into 11-cis-retinal; transport of nutrients, ions, and water; absorption of light and protection against photooxidation	2q34	The role of the <i>RPE</i> gene in lipid metabolism and inflammation is crucial in understanding the development of atherosclerosis, a major contributor to cardiovascular disease
<i>RPS7</i>	Facilitates the binding of additional ribosomal proteins to form the head of the 30S subunit by organizing the folding of the 16S rRNA 3' major domain	2p25.3	Not Directly involved

AA, Aminoacids; AKRIC3, Aldo-Keto Reductase Family 1 Member C3; CREB1, CAMP responsive element binding protein 1; CVD, cardiovascular disease; JAK3/STAT3, Janus kinases-signal transducer and activator of transcription proteins;; KLRF1, Killer Cell Lectin-Like Receptor Subfamily F Member 1; LPS, Lipopolysaccharide; LY96, Lymphocyte Antigen 96; MHC, major histocompatibility complex; NCOR2, Nuclear Receptor Corepressor 2; NMD3, NMD3 Ribosome Export Adapter; OSM, Oncostatin M; POLR2A, RNA Polymerase II Subunit A; RPE, Retinal Pigment Epithelium and RPS7, Ribosomal Protein S7; XK, XK, Kell Blood Group Complex Subunit-Related Family, Member.

Based on the findings of our investigation, it is proposed that the observed increase in the activity of specific genes (*CCL3*, *MYO18B*, *LINC00644*, *CYS1*, *CLDN8*, *RGPD4-AS1*, *LINC00958*, and *HLA-DRB5*) and the subsequent overexpression of their corresponding receptors may potentially encompass a wide array of interconnected pathways, intricately intertwined with diverse cascades such as inflammation and innate immunity.<sup>31</sup> The genes investigated in this study, along with their corresponding functions, are listed in Table 2. Prior studies have established the importance of identifying genes that are expressed differently (DEGs) in a specific ailment, as it can substantially assist in the diagnostic process.<sup>32,33</sup> Nevertheless, these 10 genes are not di-

rectly associated with the FH condition. However, this provides a potential opportunity to evaluate FH.<sup>34</sup> Through the utilization of Reverse Transcription Polymerase Chain Reaction (RT-PCR), we can examine the expression of these 10 genes in FH-affected patients to reveal their genuine influence (Fig. 6).

### Conclusions

The present investigation has identified genes that exhibit differential expression in individuals diagnosed with FH and are associated with the development of atherosclerosis compared to healthy individuals. The empirical data demonstrates a signifi-

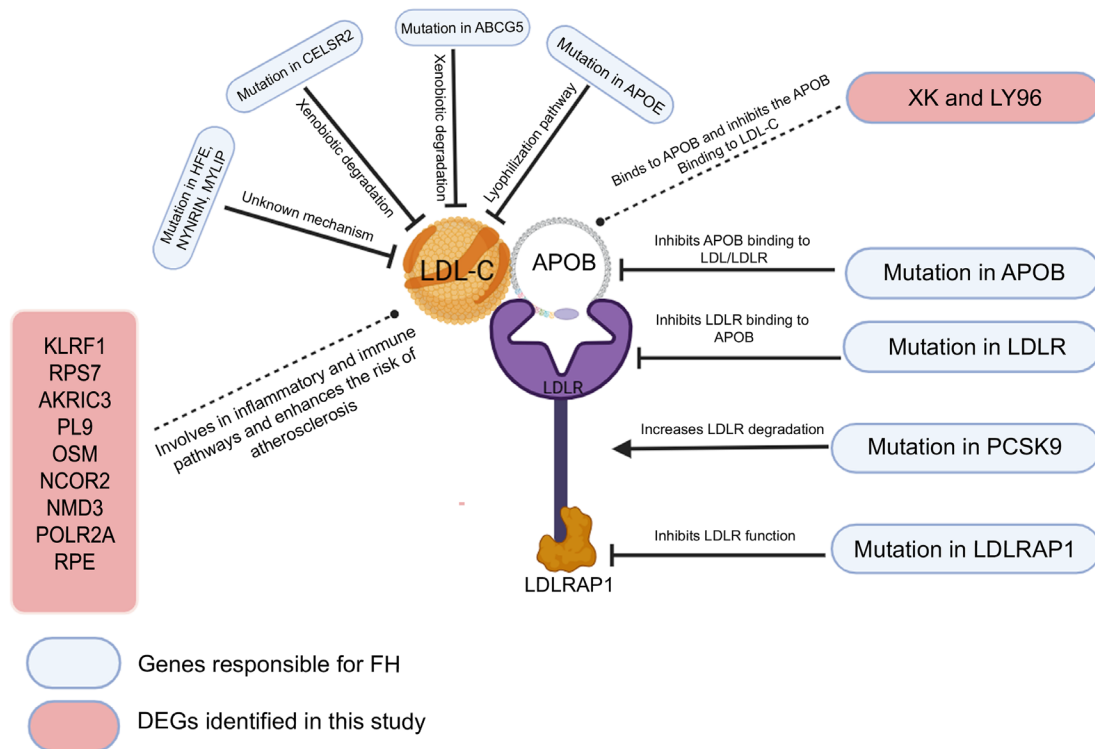


**Fig. 6. Schematic representation of genes responsible for FH and new DEGs identified in this study.** ABCG5, ATP-Binding Cassette Subfamily G Member 5; ABCG8, ATP-Binding Cassette Subfamily G Member 8; AKR1C3, Aldo-Keto Reductase Family 1 Member C3; APOB, Apolipoprotein B; APOE, Apolipoprotein E; CELSR2, Cadherin EGF LAG Seven-Pass G-Type Receptor 2; DEGs, differentially expressed genes; FH, familial hypercholesterolemia; KLRF1, Killer Cell Lectin Like Receptor F1; LDLR, Low-Density Lipoprotein Receptor; LDLRAP1, Low-Density Lipoprotein Receptor Adaptor Protein 1; LY96, Lymphocyte Antigen 96; MYLIP, Myosin Regulatory Light Chain Interacting Protein; NCOR2, Nuclear Receptor Corepressor 2; NMD3, Ribosome Exporting Factor; OSM, Oncostatin M; PCSK9, Proprotein Convertase Subtilisin/Kexin Type 9; PL9, polysaccharide lyase family 9; POLR2A, RNA Polymerase II Subunit A; RPS7, Ribosomal Protein S7; XK, X-Linked Kx Blood Group.

cant correlation between the three genes, *KLRF1*, *Xk* and *LY96*, as well as the FH genes. The genes exhibiting an elevated expression level are *RPS7*, *AKRIC3*, *PL9*, and *OSM*. These genes are of utmost importance in ribosomal transcription and the monitoring of transcription and immune responses. To enhance our comprehension of this phenomenon, the analysis of the roles of these genes in FH with atherosclerosis is necessary. The present study also establishes a foundation for investigating potential therapeutic targets that could alleviate the impact of CVD in individuals diagnosed with FH.

### Acknowledgments

All the work has been done from authors involved. KK acknowledges Department of Genetic Engineering, SRMIST for Scholar support.

### Funding

This study received no specific grant from any funding agency in the public, commercial, or not-for-profit sector.

### Conflict of interest

The authors have no conflict of interests related to this publication.

### Author contributions

KK and KNA involved in designing of the work and drafting the manuscript. JSK involved in critical revision of the paper. All authors have given approval to the final version of the manuscript.

### Data sharing statement

The data that support the findings of this study are available from the corresponding author, [Dr. KN ArulJothi], upon reasonable request. All the datasets are retrieved from NCBI Geo Datasets.

### References

- [1] ArulJothi KN, Whitthall RA, Futema M, Humphries SE, George M, Elangovan S, *et al*. Molecular analysis of the LDLR gene in coronary artery disease patients from the Indian population. *Clin Biochem* 2016;49(9):669–674. doi:10.1016/j.clinbiochem.2016.02.009, PMID: 26927322.
- [2] Reddy LL, Shah SAV, Ashavaid TF. Shortcomings on genetic testing of Familial hypercholesterolemia (FH) in India: Can we collaborate to establish Indian FH registry? *Indian Heart J* 2022;74(1):1–6. doi:10.1016/j.ihj.2021.11.185, PMID:34875256.
- [3] Pillai KKB, Shah SAV, Reddy LL, Ashavaid TF, Vishwanathan S. Targeted exome sequencing in South Indian patients with Familial hypercholesterolemia. *Clin Chim Acta* 2022;527:47–55. doi:10.1016/j.cca.2021.12.022, PMID:34998859.
- [4] EAS Familial Hypercholesterolaemia Studies Collaboration (FHSC).

- Global perspective of familial hypercholesterolaemia: a cross-sectional study from the EAS Familial Hypercholesterolaemia Studies Collaboration (FHSC). *Lancet* 2021;398(10312):1713–1725. doi:10.1016/S0140-6736(21)01122-3, PMID:34506743.
- [5] Nohara A, Tada H, Ogura M, Okazaki S, Ono K, Shimano H, *et al*. Homozygous Familial Hypercholesterolemia. *J Atheroscler Thromb* 2021;28(7):665–678. doi:10.5551/jat.RV17050, PMID:33867421.
- [6] Ashavaid TF, Todur SP, Kondkar AA, Nair KG, Shalia KK, Dalal JJ, *et al*. Platelet polymorphisms: frequency distribution and association with coronary artery disease in an Indian population. *Platelets* 2011;22(2):85–91. doi:10.3109/09537104.2010.522275, PMID:21034162.
- [7] ArulJothi KN, Suruthi Abirami B, Devi A. Genetic spectrum of low density lipoprotein receptor gene variations in South Indian population. *Clin Chim Acta* 2018;478:28–36. doi:10.1016/j.cca.2017.12.024, PMID:29269200.
- [8] McGowan MP, Hosseini Dehkordi SH, Moriarty PM, Duell PB. Diagnosis and Treatment of Heterozygous Familial Hypercholesterolemia. *J Am Heart Assoc* 2019;8(24):e013225. doi:10.1161/JAHA.119.013225, PMID:31838973.
- [9] Singh RB, Mengi SA, Xu YJ, Arneja AS, Dhalla NS. Pathogenesis of atherosclerosis: A multifactorial process. *Exp Clin Cardiol* 2002;7(1):40–53. PMID:19644578.
- [10] Harada-Shiba M. What Arteries are Affected in Familial Hypercholesterolemia? *J Atheroscler Thromb* 2019;26(12):1041–1042. doi:10.5551/jat.ED121, PMID:31645527.
- [11] Gohlke S, Zagoriy V, Cuadros Inostroza A, Méret M, Mancini C, Japtok L, *et al*. Identification of functional lipid metabolism biomarkers of brown adipose aging. *Mol Metab* 2019;24:1–17. doi:10.1016/j.molmet.2019.03.011, PMID:31003944.
- [12] Upadhyay RK. Emerging risk biomarkers in cardiovascular diseases and disorders. *J Lipids* 2015;2015:971453. doi:10.1155/2015/971453, PMID:25949827.
- [13] Jiang J, Chen H, Wang L. Gene expression analysis of familial hypercholesterolemia. *Mol Biol (Mosk)* 2014;48(1):185–192. PMID:25842839.
- [14] Reeskamp LF, Venema A, Pereira JPB, Levin E, Nieuwdorp M, Groen AK, *et al*. Differential DNA methylation in familial hypercholesterolemia. *EBioMedicine* 2020;61:103079. doi:10.1016/j.ebiom.2020.103079, PMID:33096472.
- [15] Kim SJ, Mesquita FCP, Hochman-Mendez C. New Biomarkers for Cardiovascular Disease. *Tex Heart Inst J* 2023;50(5):e238178. doi:10.14503/THIJ-23-8178, PMID:37846107.
- [16] Xuan Q, Hu C, Zhang Y, Wang Q, Zhao X, Liu X. Serum lipidomics profiles reveal potential lipid markers for prediabetes and type 2 diabetes in patients from multiple communities. *Front Endocrinol (Lausanne)* 2022;13:966823. doi:10.3389/fendo.2022.966823, PMID:36060983.
- [17] Xia J, Gill EE, Hancock RE. NetworkAnalyst for statistical, visual and network-based meta-analysis of gene expression data. *Nat Protoc* 2015;10(6):823–844. doi:10.1038/nprot.2015.052, PMID:25950236.
- [18] Zhou G, Soufan O, Ewald J, Hancock REW, Basu N, Xia J. NetworkAnalyst 3.0: a visual analytics platform for comprehensive gene expression profiling and meta-analysis. *Nucleic Acids Res* 2019;47(W1):W234–W241. doi:10.1093/nar/gkz240, PMID:30931480.
- [19] Arpino G, Generali D, Sapino A, Del Matro L, Frassoldati A, de Laurentis M, *et al*. Gene expression profiling in breast cancer: A clinical perspective. *Breast* 2013;22:109–120. doi:10.1016/j.breast.2013.01.016, PMID:23462680.
- [20] Szklarczyk D, Kirsch R, Koutrouli M, Nastou K, Mehryary F, Hachilif R, *et al*. The STRING database in 2023: Protein-protein association networks and functional enrichment analyses for any sequenced genome of interest. *Nucleic Acids Res* 2023;51(D1):D638–D646. doi:10.1093/nar/gkac1000, PMID:36370105.
- [21] Szklarczyk D, Gable AL, Nastou KC, Lyon D, Kirsch R, Pyysalo S, *et al*. The STRING database in 2021: customizable protein-protein networks, and functional characterization of user-uploaded gene/ measurement sets. *Nucleic Acids Res* 2021;49(D1):D605–D612. doi:10.1093/nar/gkaa1074, PMID:33237311.
- [22] Shannon P, Markiel A, Ozier O, Baliga NS, Wang JT, Ramage D, *et al*. Cytoscape: A Software Environment for Integrated Models of Biomolecular Interaction Networks. *Genome Res* 2003;13:2498–2504. doi:10.1101/gr.1239303, PMID:14597658.
- [23] Awan Z, Alrayes N, Khan Z, Almansouri M, Ibrahim Hussain Bima A, Al-mukadi H, *et al*. Identifying significant genes and functionally enriched pathways in familial hypercholesterolemia using integrated gene co-expression network analysis. *Saudi J Biol Sci* 2022;29(5):3287–3299. doi:10.1016/j.sjbs.2022.02.002, PMID:35844366.
- [24] Kuleshov MV, Jones MR, Rouillard AD, Fernandez NF, Duan Q, Wang Z, *et al*. Enrichr: a comprehensive gene set enrichment analysis web server 2016 update. *Nucleic Acids Res* 2016;44(W1):W90–97. doi:10.1093/nar/gkw377, PMID:27141961.
- [25] Chen EY, Tan CM, Kou Y, Duan Q, Wang Z, Meirelles GV, *et al*. Enrichr: interactive and collaborative HTML5 gene list enrichment analysis tool. *BMC Bioinformatics* 2013;14:128. doi:10.1186/1471-2105-14-128, PMID:23586463.
- [26] Wang D, Liu B, Xiong T, Yu W, She Q. Investigation of the underlying genes and mechanism of familial hypercholesterolemia through bioinformatics analysis. *BMC Cardiovasc Disord* 2020;20(1):419. doi:10.1186/s12872-020-01701-z, PMID:32938406.
- [27] Xie Z, Bailey A, Kuleshov MV, Clarke DJB, Evangelista JE, Jenkins SL, *et al*. Gene Set Knowledge Discovery with Enrichr. *Curr Protoc* 2021;1(3):e90. doi:10.1002/cpz1.90, PMID:33780170.
- [28] Vaezi Z, Amini A. Familial Hypercholesterolemia. *StatPearls. Treasure Island (FL): StatPearls Publishing; 2024*. PMID:32310469.
- [29] Jung HH, Danek A, Walker RH, Frey BM, Peikert K. McLeod Neuroacanthocytosis Syndrome. In: Adam MP, Feldman J, Mirzaa GM, Pagon RA, Wallace SE, Bean LJH (eds). *GeneReviews®*. Seattle (WA): University of Washington; 2004. PMID:20301528.
- [30] Lancaster GI, Langley KG, Berglund NA, Kammoun HL, Reibe S, Estevez E, *et al*. Evidence that TLR4 Is Not a Receptor for Saturated Fatty Acids but Mediates Lipid-Induced Inflammation by Reprogramming Macrophage Metabolism. *Cell Metab* 2018;27:1096–1110.e5. doi:10.1016/j.cmet.2018.03.014, PMID:29681442.
- [31] Bekenev VA, Arishin AA, Mager SN, Bolshakova I V, Tretyakova NL, Kashtanova EV, *et al*. Lipid Profile of Pig Tissues Contrasting in Meat Production. *Nat Prod J* 2021;11:108–118. doi:10.2174/2210315509666191203124902.
- [32] Torabi F, Vadakekolathu J, Wyatt R, Leete P, Tombs MA, Richardson CC, *et al*. Differential expression of genes controlling lymphocyte differentiation and migration in two distinct endotypes of type 1 diabetes. *Diabet Med* 2023;40(9):e15155. doi:10.1111/dme.15155, PMID:37246834.
- [33] Zhang W, Long H, He B, Yang J. DEctP: Calling Differential Gene Expression Between Cancer and Normal Samples by Integrating Tumor Purity Information. *Front Genet* 2018;9:321. doi:10.3389/fgene.2018.00321, PMID:30210526.
- [34] Ekroos K, Lavrynenko O, Titz B, Pater C, Hoeng J, Ivanov NV. Lipid-based biomarkers for CVD, COPD, and aging - A translational perspective. *Prog Lipid Res* 2020;78:101030. doi:10.1016/j.plipres.2020.101030, PMID:32339553.